LATVIAN JOURNAL OF PHYSICS AND TECHNICAL SCIENCES
2015, N 5

DOI: 10.1515/LPTS-2015-0025

SOLID STATE PHYSICS

THE KINETIC STUDY OF THE HYDROTHERMAL GROWTH OF ZnO NANOROD ARRAY FILMS

V.Gerbreders, P. Sarajevs, I.Mihailova, E. Tamanis

G. Liberts' Innovative Microscopy Centre, Daugavpils University
1 Parades Str., LV-5401, Daugavpils, LATVIA
e-mail: vjaceslavs.gerbreders@du.lv

The simple analysis method has been introduced for the kinetic analysis of the hydrothermal growth. The zinc oxide nanorod arrays have been synthesized via a hydrothermal process. Zinc nitrate hexahydrate ($Zn(NO_3)_2 \cdot 6H_2O$) has been used as the precursor in the presence of hexamethylenetetramine ($C_6H_{12}N_4$) for the formation of ZnO nanostructures. Long-term isothermal growth kinetics of ZnO nanorods has been investigated. The effect of the solution temperature (70–90 °C) on the kinetics of the hydrothermal growth of ZnO nanorods has been examined. An extensive analysis by scanning electron microscopy, energy dispersive spectroscopy and x-ray diffraction has revealed that the as-synthesized ZnO nanorod arrays are well-crystalline and possessing hexagonal wurtzite structure. These ZnO films have promising potential advantages in microelectronic and optoelectronic applications.

Keywords: *hydrothermal crystal growth, kinetics, nanorods, nanostructures, semiconductor, ZnO.*

1. INTRODUCTION

The studies on zinc oxide (ZnO) nanostructures have been intensified worldwide in the past two decades. Synthesis of size and shape controlled nanostructures (wires, rods, fibres, tubes, spheres, tetrapods and multipods, triangles, cubes etc.), their properties and possible applications are under rigorous research. Combination of unique optical, mechanical and piezoelectrical properties makes ZnO a prospective material for a variety of applications in electronics, optoelectronics and magnetoelectronics. The application of ZnO nanostructures as different sensors [1], [2], [3], piezoelectric elements [4] and generators [5], solar cells [6], [7], opens up new possibilities in diagnostics, microelectronics, photovoltaics etc.

Many different synthesis methods have been developed to generate ZnO nanostructures with different morphology. The hydrothermal growth method has attracted increasing attention due to its simplicity, efficiency and environmentally friendly conditions. This method allows us to create a large-scale area of well-aligned ZnO

nanorod (NR) arrays [8], as well as to carry out the area-selective growth of nanostructures with controllable structural properties [9], [10]. The size and shape of the nanostructures depend on various factors, such as seed layer parameters, chemical composition, temperature, acidity of precursors etc. For example, a change in the solution temperature during the hydrothermal growth can transform ZnO nanorods into ZnO nanotubes [11] or change the conductivity type of the sample [12], [13]. Due to such a variety of influencing factors, a detailed study of the hydrothermal growth processes of nanostructures is required to create nanorods with the necessary parameters. An understanding of kinetics of the crystallisation process is important for the selection of processing parameters, such as temperature, chemical composition etc. To analyse the isothermal crystallisation processes, typically the Avrami Erofeeva equation [14]:

$$\alpha = 1 - e^{(-kt^n)} \tag{1}$$

or parabolic kinetic equation is used [15], [16], [17]:

$$D^n - D_0^n = kt, \tag{2}$$

where α is the fractional decomposition, t is the time, k is a rate constant and n – the parameter, which determines the nucleation and growth mode; D is the average grain size after growth for time t, D_0 – the initial grain size, k is a temperature dependent parameter and can be expressed in an Arrhenius-type equation:

$$k = k_0 e^{\left(\frac{-E_a}{k_B T}\right)}, \tag{3}$$

where E_a is the activation energy and k_B – the Boltzmann constant.

In our case, due to a high density of the nanorods in the samples, the growth kinetics of nanorods can be considered the growth kinetics of homogeneous thin film of zinc oxide; therefore, it is more convenient to use (2), where D is the average length of ZnO nanorods, which also is equivalent to the thickness of the film. Since D_0 is always very small, Eq. (2) can be rewritten as follows:

$$D^n = kt\,, \tag{4}$$

2. EXPERIMENTAL PART

ZnO nanorod arrays have been prepared on microscopic glass substrates by catalyst-free two-step processing: (a) preparation of ZnO seed layer and (b) growth of ZnO nanorod arrays. In the first step, ZnO precursor films have been deposited onto pre-cleaned glass substrates by direct current magnetron *sputtering (Kurt Lesker LAB18)* using *ZnO:Al* (99 % ZnO, 1 % Al) target in a vacuum. The thickness of the obtained films is approximately 30 nm. Sputtering has been carried out perpendicular to the substrate in order to obtain a well-aligned ZnO nanorod array [18].

At the second stage, the synthesis of hexagonal ZnO nanorods has been carried out using the hydrothermal growth method. The seeded substrates have been placed inverted (with the growth-side downwards) in thermostat containing an aqueous solution of 0.05 M zinc nitrate hexahydrate ($Zn(NO_3)_2 \cdot 6H_2O$; 99 % purity) and 0.05 M hexamethylenetetramine ($C_6H_{12}N_4$; 99 % purity). Schematic diagram of the experimental setup is shown in Fig. 1. The constant temperature at 70, 75, 80, 85 and 90 °C has been maintained for a certain time. The growth process has been carried out using a laser scanning confocal microscope Leica to record the interference pattern at a wavelength of 632.8 nm. Laser beam (1) scans the surface of sample (2) and captures the surface image at a certain time t. Over time growth of ZnO nanorod, array occurs, which for the laser beam with a diameter of 0.9 mm can be considered a homogeneous film. At normal incidence of laser beam condition for the reflected signal maxima is

$$2dN = m\lambda, \qquad \text{m} = 1, 2\ldots, \tag{5}$$

where d represents the thickness of the layer, N is the refractive index of the layer, l is the light wavelength, m is an integer. Rearranging Eq. (4) to solve for thickness d gives

$$d = \frac{m\lambda}{2N}. \tag{6}$$

If refractive index N (N=1.9888) and wavelength λ (λ=632.8 nm) are known and m is the number of peak maxima between experimentally measured interference peaks, the layer thickness can be calculated from Eq. (6). In our case, d is equal to the length of ZnO nanorods (d=D). Thus, this interference technique allows determining changes in the length of nanorods over time.

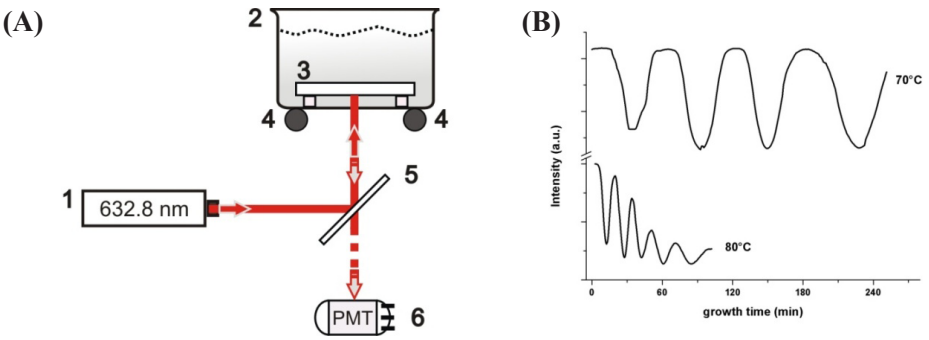

Fig. 1. (a) Schematic diagram of the experimental setup: 1–He-Ne laser with 632.8 nm CW Output, 2 – thermostat, 3 – sample, 4 – heater, 5 – beam splitter, 6 – photomultiplier; (b) The interference pattern obtained during ZnO film deposition at temperatures of 70 and 80 °C.

The obtained samples have then been rinsed with distilled water and dried with a N_2 gun for characterisation. The surface morphology and structural properties have been studied using a scanning electron microscopy (SEM, *TESCAN-VEGA*

LMU II operated at 30kV) and X-ray diffraction (XRD, SmartLab RIGAKU diffractometer with Cu-Kα (λ=1.543 Å)), respectively. The obtained X-ray pattern peaks have been compared to the ones from the data base [19].

3. RESULTS AND DISCUSSION

All the as-grown ZnO nanorod arrays are well aligned with strongly (002) preferential orientation along the c-axis of the substrate and have strong texture (Fig. 2).

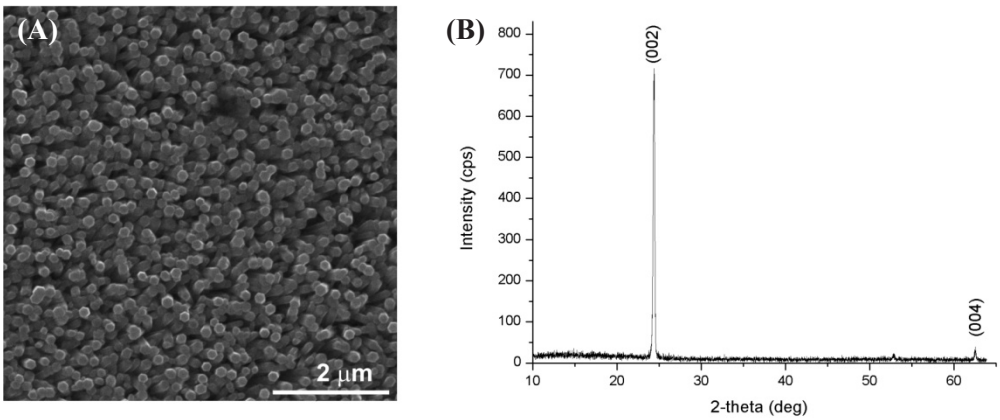

Fig. 2. (a) SEM image and (b) XRD pattern of ZnO film obtained at 80 °C.

The isothermal crystallisation kinetics has been studied at different temperatures. Based on the interference fringes (Fig. 1), the crystallisation process has been observed as the growth of individual hexagonal nanorods with direction (002). The length of nanorods has been calculated from Eq. (6). Plot of ZnO NRs length D versus time during the isothermal crystallisation process at different temperatures is shown in Fig. 3.

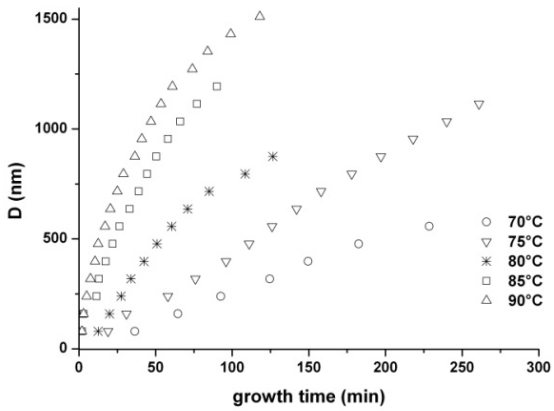

Fig. 3. Plot of ZnO NRs length versus time.

The logarithmic form of Eqs. (3) and (4) is represented as Eq. (7):

$$\ln D = \frac{1}{n} \cdot \frac{E_\alpha}{k_B} \cdot \frac{1}{T} + \frac{1}{n} \ln t + \frac{1}{n} \ln k_0 \ , \tag{7}$$

$$\ln t = n \ln D - \ln k_0 - \frac{E_\alpha}{k_B} \cdot \frac{1}{T} \ . \tag{8}$$

The crystallisation kinetic parameters during the isothermal process have been determined according to these equations. The values of D and t, derived from the relationship shown in Fig. 3, are a linear function ln (D) from ln (t) (Fig. 4) described by Eq. (7). Then, at a constant temperature slope of the straight line is associated with the exponent n by ratio n = 1/tg (β) (Fig. 4). The n values shown in Fig. 4 depend on the temperature and are in the range from 0.92 to 1.5.

According to [20], there is a certain relation between the value of n and the mechanism of crystallisation and while in the range from 1 to 2 the process of crystallisation can be characterised as one-dimensional crystal growth. In our case, n ranges from 0.92 to 1.50, which corresponds to a one-dimensional growth of hexagonal rods with direction (002). Withal, Jing-Jing Dong et al. [21] studied the influence of the reaction temperature and solution concentration on the hydrothermal growth of ZnO nanorods; they revealed that the length of ZnO nanorods depended mainly on the reaction temperature, while the diameter was closely related with the solution concentration. In our case, the seed layer and the solution concentration are similar for all samples, and the influence of growth temperature on the growth kinetic has been studied. The above-mentioned results confirm that our method is suitable for kinetic analysis of one-dimensional crystal growth.

The values of t and D, derived from the relationship shown in Fig. 3, are a linear function ln (t) from 1/T (Fig. 5), which is described by Eq. (8). The activation energy derived from Eq. (8) is $E_a = k_B \cdot tg\,(\alpha) = 123$ kJ/mol.

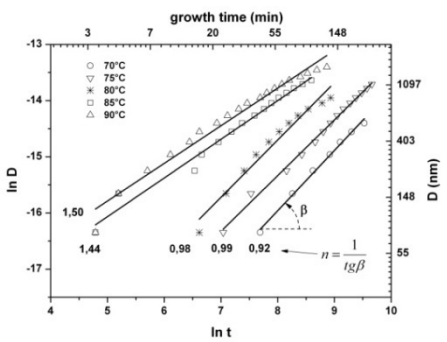

Fig. 4. Plot of ln (D) vs ln (t).

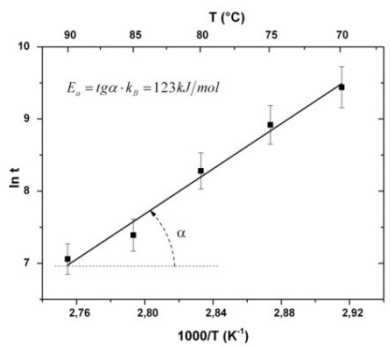

Fig. 5. Plot of ln (t) vs 1000/T.

The authors of [22] consider the hydrothermal growth of ZnO crystals to be a process consisting of two parts. One is the diffusion process of the reactants to the

surface of the growing crystallite, while the second one is the reaction at the surface of the crystallite to incorporate the reactant as part of the growth process. Both these processes had been taken into consideration in the modelling of the growth process. The authors estimated concentration-independent activation energy of 0.735 eV (70.9 кJ/mol). In the paper [23], considering the hydrothermal growth of ZnO to be a one-dimensional growth, the authors obtained the activation energy of 96.12 kJ/mol. The activation energy for forming ZnO crystals during the annealing of amorphous film in the temperature range from 100 to 500 °C is from 22 to 24 kJ/mol [16], 234 kJ/mol – for the synthesis of nanowires by thermal chemical vapour [24].

Our value of the activation energy is in a very good agreement with experimental data given in the above-mentioned literature. This demonstrates the applicability of the experimental technique we use for the study of one-dimensional crystal growth of ZnO nanostructures. Furthermore, the ability to scan a user-defined area of the sample is useful for studying various local kinetic parameters during hydrothermal growth.

4. CONCLUSIONS

The simple analysis method has been introduced for the kinetic analysis of the hydrothermal growth. In situ thin film thickness monitoring has been implemented. Technique is based on measuring the reflection of a laser beam from the film–substrate system; the interference pattern obtained during film deposition has been used to calculate the film thickness. The parabolic kinetics law has been applied to describe the isothermal crystallisation process of ZnO nanorods. The activation energy for the hydrothermal growth of ZnO nanorod array has been determined to be 123 kJ/mol. This method is suitable for one-dimensional growth analysis and opens up new perspectives for further investigation.

ACKNOWLEDGEMENTS

ESF EIROPAS SOCIĀLAIS FONDS
IEGULDĪJUMS TAVĀ NĀKOTNĒ

The present research has been supported by ESF Project No. 2013/0029/1DP/1.1.1.2.0/13/APIA/VIAA/029.

REFERENCES

1. Tang, W., and Wang, J. (2015). Mechanism for toluene detection of flower-like ZnO sensors prepared by hydrothermal approach: Charge transfer. *Sensors and Actuators B, 207*, 66–73.
2. Wei, A., Pan, L., and Huang, W. (2011). Recent progress in the ZnO nanostructure-based sensors. *Materials Science and Engineering B, 176,* 1409–1421.
3. Arya, S.K., Saha, S., Ramirez-Vick, J. E., Gupta, V., Bhansali, S., and Singh, S.P. (2012). Recent advances in ZnO nanostructures and thin films for biosensor applications: Review. *Analytica Chimica Acta, 737*, 1–21.
4. Pan, C.T., Chen, Y.C., Hsieh, C.C., Lin, C.H., Su, C.Y., Yen, C.K., Liu, Z.H., and Wang, W.C. (2014). Ultrasonic sensing device with ZnO piezoelectric nanorods by selectively electrospraying method. *Sensors and Actuators A: Physical, 216,* 318–327.

5. Wang, X. (2012). Piezoelectric nanogenerators – Harvesting ambient mechanical energy at the nanometer scale. *Nano Energy, 1,* 13–24.
6. Tang, Z., Koshino, H., Sato, S., Shimizu, H., and Shirai, H. (2012). Rapid thermal annealing treatment of ZnO: Al films for photovoltaic applications. *Journal of Non-Crystalline Solids, 358,* 2501–2503.
7. Guérin, V. M., Rathousky, J., and Pauporté, Th. (2012). Electrochemical design of ZnO hierarchical structures for dye-sensitized solar cells. *Solar Energy Materials and Solar Cells, 102,* 8–14.
8. Zou, X., Fan, H., Tian, Y., and Yan, S. (2013). Facile hydrothermal synthesis of large scale ZnO nanorod arrays and their growth mechanism. *Materials Letters, 107,* 269–272.
9. Zhitao, H., Sisi, L., Jinkui, C., and Yong, C. (2013). Controlled growth of well-aligned ZnO nanowire arrays using the improved hydrothermal method. *Journal of Semiconductors, 34,* 063002-1-16.
10. Hong, S., Yeo, J., Manorotkul, W., Kang, H. W., Lee, J., Han, S., Rho, Y., Suh, Y. D., Sung, H. J., and Hwan Ko, S. (2013). Digital selective growth of a ZnO nanowire array by large scale laser decomposition of zinc acetate. *Nanoscale, 5,* 3698–3703.
11. Huang, B.R., and Lin, J.C. (2013). A facile synthesis of ZnO nanotubes and their hydrogen sensing properties. *Applied Surface Science, 280*, 945–949.
12. Hsu, Y.F., Xi, Y.Y., Tam, K.H., Djurišić, A.B., Luo, J., Ling, C.C., Cheung, C.K., Ching, A.M., Chan, W.K., Deng, X., Beling, C.D., Fung, S., Cheah, K.W., Keung Fong, P.W., and Surya, C.C. (2008). Undoped p-Type ZnO Nanorods Synthesized by a Hydrothermal Method. *Advanced Functional Materials, 18(7),* 1020–1030.
13. Lu, M.P., Lu, M.Y., and Chen, L.J. (2012). p-Type ZnO nanowires: From synthesis to nanoenergy. *Nano Energy, 1,* 247–258.
14. Vallejo, W., Hurtado, M., and Gordillo, G. (2010). Kinetic study on Zn(O,OH)S thin films deposited by chemical bath deposition. *Electrochimica Acta, 55,* 5610–5616.
15. Singh, R.G., Singh, F., Kumar, V., and Mehra, R.M. (2011). Growth kinetics of ZnO nanocrystallites: Structural, optical and photoluminescence properties tuned by thermal annealing. *Current Applied Physics, 11,* 624–630.
16. Bouhssira, N., Aida, M.S., Mosbah, A., and Cellier, J. (2010). Isothermal crystallization kinetic of ZnO thin films. *Journal of Crystal Growth, 312,* 3282–3286.
17. Ko, H.H., Hsi, C.S., Wang, M.C., and Zhao, X. (2014). Crystallite growth kinetics of TiO_2 surface modification with 9 mol% ZnO prepared by a coprecipitation process. *Journal of Alloys and Compounds, 588,* 428–439.
18. Mihailova, I., Gerbreders, V., Bulanovs, A., Tamanis, E., Sledevskis, E., Ogurcovs, A., and Sarajevs, P. (2014). Controlled growth of well-aligned ZnO nanorod arrays by hydrothermal method. *Proc. of SPIE Vol. 9421,* 94210A1-8.
19. Altomare, A., Camalli, M., Cuocci, C., Giacovazzo, C., Moliterni, A., and Rizzi, R. (2009). EXPO2009: Structure solution by powder data in direct and reciprocal space. *Appl. Cryst. 42,* 1197–1202.DOI:10.1107/S0021889809042915.
20. Mandelkern, L. (1958). *Growth and Perfection of Crystals*, in R. H. Doremus, B.W. Roberts, and D. Turnbull eds. New York: John Wiley & Sons Inc., pp. 467–474.
21. Dong, J.J., Zhen, C.Y., Hao, H.Y., Xing, J., Zhang, Z.L., Zheng, Z.Y., and Zhang, X.W. (2013). Controllable synthesis of ZnO nanostructures on the Si substrate by a hydrothermal route. *Nanoscale Res. Lett. 8(1),* 378.
22. Viswanatha, R., Santra, P.K., Dasgupta, C., and Sarma, D.D. (2007). Growth mechanism of nanocrystals in solution: ZnO, a case study. *Phys. Rev. Lett. 98,* 255501.

23. Feng, W., and Huang, P. (2014). A generalized mechanism of 1D ZnO rods growth in homogeneous solution. *Ceramics International, 40,* 8963–8967.
24. Yang, Y.H., and Yang, G.W. (2010). Temperature dependence and activation energy of ZnO nanowires grown on amorphous carbon. *Chemical Physics Letters, 494,* 64–68.

ZnO NANOSTIEŅU KOPU PĀRKLĀJUMA HIDROTERMĀLĀS AUGŠANAS KINĒTIKAS IZPĒTE

V. Gerbreders, P. Sarajevs, I. Mihailova, E. Tamanis

K o p s a v i l k u m s

Tiek piedāvāta vienkārša analīzes metode kristālu hidrotermālās augšanas kinētikasizpētei. Labi sakārtotu ZnO nanostieņu kopa tika sintezēta pielietojot hidrotermālās augšanas metodi, cinka nitrāta heksahidrāta ($Zn(NO_3)_2 \cdot 6H_2O$) un heksametilēntetramīna ($C_6H_{12}N_4$) šķīdumā. Plānās kārtiņas biezuma izmaiņas tika novērotas reālā laikā, pielietojot interferometrijas tehniku. Tika mērīts no sistēmas plānā kārtiņa – pamatne atstarotais lāzerstars; iegūtā interferences aina tika izmantota plānās kārtiņas biezuma aprēķiniem. ZnO nanostieņu izotermiskās kristalizācijas procesa kinētika tika aprakstīta ar parabolisku likumu. Tika aprēķināts, ka ZnO nanostieņu kopu hidrotermālās augšanas aktivācijas enerģija ir 123kJ/mol. Šī metode ir piemērota viendimensionālas augšanas procesu analīzei un paver jaunas iespējas turpmākiem pētījumiem.

26.05.2015.